www.ietdl.org

Published in IET Microwaves, Antennas & Propagation
Received on 19th October 2011
Revised on 7th March 2012
doi: 10.1049/iet-map.2011.0492

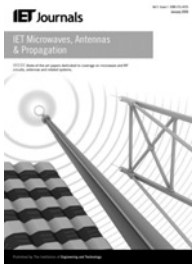

ISSN 1751-8725

Concentric circular-shaped electronically steerable parasitic array radiator antennas for full-azimuth directions of arrival estimation with reduced computational load

S. Akkar F. Harabi A. Gharsallah

Faculty of Sciences of Tunis, Unit of Research in High Frequency Electronic Circuits and Systems, El Manar University, 2092 Tunis, Tunisia
E-mail: salemakkar@yahoo.fr

Abstract: This study proposes a new uniform concentric circular (UCCA) shape of electronically steerable parasitic array radiator (ESPAR) antennas for directions of arrival (DoAs) estimation problem. The well-known estimation of signal parameters via rotational invariance techniques (ESPRIT) algorithm is adapted to this special shape of UCCA and the authors demonstrate that the resulting algorithm yields better DoAs estimation accuracy and solves the failure of estimation problem when the signals' DoAs are in some particular sectors: notably for [0°–30°] and [160°–180°]. This approach has shown interesting performances since it can ensure good DoAs estimation over the entire azimuth plane with a low extra computational overhead. The constraints are the same imposed to the ESPRIT algorithm allowing about 66% reduction on the required computational efforts. The Cramer Rao bound on the variance of DoAs estimated by the proposed array geometry is analysed. Through simulation results, the authors demonstrate that applying ESPRIT in conjunction with the proposed antennas shape not only provides superior high-resolution localisation capabilities but also it drastically reduces computations compared with previous works.

1 Introduction

Estimating the directions of arrivals (DoAs) of several signals impinging on a sensor array is a challenging problem in many applications including radar, sonar, personal location and mobile communications. High-resolution DoAs estimators such as multiple signal classification (MUSIC), estimation of signal parameters via rotational invariance techniques (ESPRIT) and Propagator [1–3] have received considerable attention because of their good resolution and are among the most efficient methods for DoAs estimation. Recently, efforts have been focused on DoAs estimation through the use of electronically steerable parasitic array radiator (ESPAR) antennas systems. This new kind of antennas arrays consists of one fed active element surrounded by some parasitic radiating elements placed in the near field of the active radiator and working near resonance. ESPAR antennas systems, that have received an increasing attention recently [4–10], present many advantages over conventional arrays such as a low-power consumption (only the active element is fed), a low cost (only one analogue-to-digital converter (ADC) placed in the output of active element), a small-size (because they are fundamentally based on the mutual coupling phenomenon) and an easy fabrication. Furthermore, the low-power consumption in comparison with conventional arrays makes the ESPAR antennas very suitable for mobile applications since they can ensure more energetic autonomy, which is always demanded in such applications. The seven-element hexagonally shaped ESPAR antenna is first proposed in [6] for DoAs estimation. However, the achieved performance depends strongly on the signals DoAs. In [7], based on simultaneous use of three pairs of subarrays, another method that can be also directly applied with our proposed ESPAR antennas shape is introduced. Moreover, the enhanced reactance domains ESPRIT algorithm (Enhanced-RD-ESPRIT) proposed in [8], which uses a generalised reactance domains (RD) covariance matrix obtained with a large number of beam patterns compared with the parasitic antennas elements number, improves the DoAs estimation in the full azimuth plane. However, since the number of beam patterns define the size of the resulting RD covariance matrix, this size increases with the number of beam patterns and, thus, both calculation load and processing time of the DoAs estimator increase as well. One of the most popular antennas array shapes is the uniform circular array because it has several advantages over other schemes such as the beam patterns that can be kept invariant, a certain degree of source elevation information and all azimuth scan capability (it can perform 360° scan around its centre). The ESPAR antennas data is collected by the RD technique that requires directive radiation patterns to reduce the estimation errors

on the data covariance matrix. Since it is able to form directive radiation patterns, circular shaped ESPAR antennas are often used for DoAs estimation. However, not all DoAs estimation algorithms developed for linear arrays (e.g. ESPRIT algorithm) can be easily applied to any antenna array shape for either mathematical or computational reasons.

In this paper, we propose a new uniform concentric circular (UCCA) shape of ESPAR antennas to improve DoAs estimation accuracy regardless of the sources angular positions. This new ESPAR antenna shape takes full advantage of common planar and circular arrays. First, it keeps the circular shape overview of the ESPAR antenna system, which reduces the data covariance matrix estimation errors by means of the directive radiation patterns that can be formed. Second, it guarantees an accurate DoAs estimation in the entire half-azimuth plane since two identical circular subarrays, required to execute the ESPRIT algorithm, can be found in its special geometrical structure. Thus, the advantage of the proposed UCCA ESPAR antennas is two-fold. First, the failure estimation problem, that prohibits the full-azimuth coverage, can be solved since the circular array shape is known by its full-azimuth scan capability. Second, the calculation costs and complexity are reduced by at least a factor of three since only one singular values decomposition (SVD) computation is required to cover the entire half-azimuth plane instead of three as in [6, 8]. Therefore applying ESPRIT algorithm in conjunction with the proposed ESPAR antennas shape will yield to about 66% of calculation cost reduction over existing schemes, which constitutes a challenging criterion for a real-time implementation of any DoAs estimator (e.g. as on a DSP chip).

The paper outline is as follows. Section 2 describes the new ESPAR antennas shape and the used data model. Section 3 details the DoAs estimation procedure. Section 4 is devoted to analyse the complexity and the calculation cost of the DoAs estimator. Section 5 shows the performances on DoAs estimation of the proposed ESPAR antennas shape through a series of computer simulations. Section 6 concludes the paper.

In this paper, the superscripts $(.)^{\mathrm{T}}$, $(.)^{*}$, $(.)^{\mathrm{H}}$, $(.)^{-1}$, and $(.)^{\dagger}$ are the matrix transpose, conjugate, Hermitian, inverse and the pseudo-inverse operators, respectively.

2 System model

2.1 Proposed ESPAR antenna shape (UCCA)

The proposed ESPAR antennas configuration is composed of one active element (#1) surrounded by $M = 6$ parasitic elements (#2–#7) distributed over two rings and loaded with variable reactances x_m ($m = 1$ to M) as shown in Fig. 1. The first ring is composed of $P = 4$ parasitic elements; however, the second ring is composed of only two parasitic elements and all are assumed to be identical. In the presence of K impinging narrowband signals from K distinct DoAs ($\theta_1, \theta_2, \ldots, \theta_K$) the steering matrix is given as

$$\boldsymbol{A} = \begin{bmatrix} \boldsymbol{A}_1 \\ \boldsymbol{A}_2 \end{bmatrix} \tag{1}$$

where

$$\boldsymbol{A}_1 = [\boldsymbol{a}_1(\theta_1), \boldsymbol{a}_1(\theta_2), \ldots, \boldsymbol{a}_1(\theta_K)] \tag{2}$$

$$\boldsymbol{A}_2 = [\boldsymbol{a}_2(\theta_1), \boldsymbol{a}_2(\theta_2), \ldots, \boldsymbol{a}_2(\theta_K)] \tag{3}$$

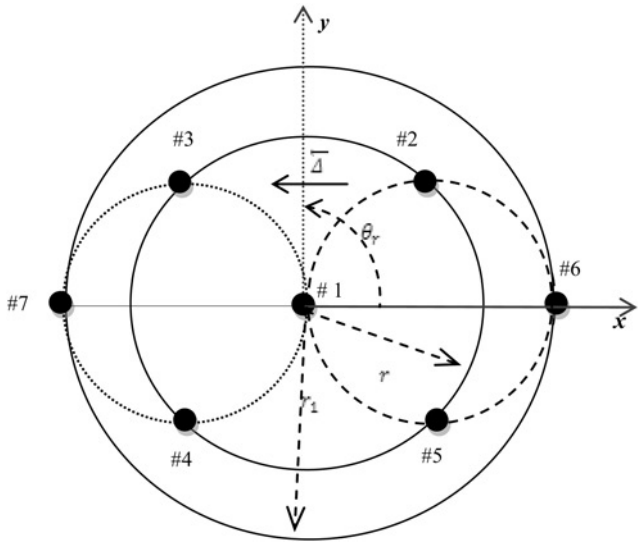

Fig. 1 *Top view of the proposed UCCA–ESPAR antennas: the subarrays are drawn with dotted and dashed lines, respectively, whereas the invariance translation direction is designed by* $\boldsymbol{\Delta}^{\rightarrow}$

$$\boldsymbol{a}_1(\theta_k) = \left[1, \mathrm{e}^{\mathrm{j}(2\pi r/\lambda)\cos(\theta_k - \varphi_1)}, \ldots, \mathrm{e}^{\mathrm{j}(2\pi r/\lambda)\cos(\theta_k - \varphi_P)}\right]^{\mathrm{T}}$$

$$\boldsymbol{a}_2(\theta_k) = \left[\mathrm{e}^{\mathrm{j}(2\pi r_1/\lambda)\cos(\theta_k)}, \mathrm{e}^{\mathrm{j}(2\pi r_1/\lambda)\cos(\theta_k - \pi)}\right]^{\mathrm{T}}$$

with $\varphi_p = (2\pi/P)(p-1) + (\pi/4)$; for $p = 1$ to P.

As illustrates Fig. 1, the seven-elements UCCA-ESPAR antennas can be decomposed in two identical circular subarrays required to execute the ESPRIT algorithm. The translational invariance $\boldsymbol{\Delta}$ between these subarrays acts in the same way as with a linear antenna array and it refers to the fact that one subarray can be obtained from the translation of the other. Therefore the spatial delay between subarrays 1 and 2 because of displacement invariance $\boldsymbol{\Delta}$ leads to a phase delay β_k on the incoming signal $S_k(t)$ expressed as

$$\beta_k = \mathrm{e}^{j\mu_k} = \mathrm{e}^{\mathrm{j}(2\pi/\lambda)\|\Delta\|\sin(\theta_k - \theta_{\mathrm{r}})} \tag{4}$$

where $\theta_{\mathrm{r}} = \pi/2$ is a constant angle of reference.

The radius of the external ring is fixed to a quarter wavelengths ($r_1 = \lambda/4$) and the radius of the internal ring is chosen with respect of an array geometry that offers us two identical uniform circular subarrays (e.g. $r = r_1/\sqrt{2}$).

2.2 Data model

Since the data are available only in the output of the active element, an additional assumption about sources is required to form our data covariance matrix from observation available only in the output of the active element. Indeed, the K incident sources are assumed to be sent periodically from the far field. Although the signals are periodically sent, as many times as the number of the used directional radiation patterns (e.g. $M+1$ time), the received scalar output signal from the active element $y(t_m)$ is stocked into a vector $\boldsymbol{Y}(t)$. By changing the parasitic elements reactance values under $M+1$ periods (accordingly we change the radiation patterns of the ESPAR antennas $M+1$ times), we can obtain our data vector $\boldsymbol{Y}(t)$. Therefore the spatial diversity of conventional array is recreated by periodically changing the reactance values and, thus, the radiation

patterns of the ESPAR antennas: this diversity is also called the angular diversity. This technique is known in signal processing as the RD technique [5]. The assumption of periodic signals allows us to write

$$S_k(t_1) = S_k(t_2) = \cdots = S_k(t_{M+1}) \tag{5}$$

where we denote by $S_k(t_m)$ the complex magnitude of the kth incoming periodic signal at the instant t_m. In this case, the received signal vector $\boldsymbol{Y}(t)$ by the ESPAR antennas can be written as

$$\boldsymbol{Y}(t) = [y(t_1), y(t_2), \ldots, y(t_{M+1})]^{\mathrm{T}}$$

$$\text{with } y(t_1) = \sum\nolimits_{k=1}^{K} \boldsymbol{w}_1^{\mathrm{T}} \boldsymbol{a}(\theta_k) S_k(t_1) + n(t_1) \tag{6}$$

The frequency weighed matrix $\boldsymbol{W}$ is given as: $\boldsymbol{W} = [\boldsymbol{w}_1^{\mathrm{T}}, \boldsymbol{w}_2^{\mathrm{T}}, \ldots, \boldsymbol{w}_{M+1}^{\mathrm{T}}]^{\mathrm{T}}$ and each one of its components is computed as

$$\boldsymbol{w}_m = 2Z_s(\boldsymbol{Z} + \boldsymbol{X}^{(m)})^{-1}\boldsymbol{u} \tag{7}$$

where Z_s is the receiver's input impedance; $\boldsymbol{u} = [1, 0, 0, \ldots, 0]^{\mathrm{T}}$; $\mathbf{Z} \in \mathbb{C}^{(M+1)\times(M+1)}$ is the mutual impedances matrix.

$\boldsymbol{X}^{(m)}$ is a diagonal matrix that contains the mth set of reactance (for $m = 1$ to $M + 1$) and it is given as

$$\boldsymbol{X}^{(m)} = \mathrm{diag}\{Z_s, jx_1^{(m)}, jx_2^{(m)}, \ldots, jx_M^{(m)}\} \tag{8}$$

In matrix notation, the received data vector by the ESPAR antennas can be given as

$$\boldsymbol{Y}(t) = \boldsymbol{W}^{\mathrm{T}}\boldsymbol{A}\boldsymbol{S}(t) + \boldsymbol{N}(t) \tag{9}$$

where $\boldsymbol{N}(t) = [n(t_1), n(t_2), \ldots, n(t_{M+1})]^{\mathrm{T}}$ refers to an additive Gaussian noise vector assumed to be spatially white and zero mean (e.g. $E[\boldsymbol{N}\boldsymbol{N}^{\mathrm{H}}] = \sigma^2\boldsymbol{I}$).

Under assumption that the noise and the signals are not correlated with each other (e.g. for $\forall\ i, j$; $E[s_i n_j^*] = 0$ and $\forall\ i \neq j$, $E[s_i s_j^*] = 0$) the estimated (sampled) covariance matrix, obtained through N_s snapshots, can be given as

$$\hat{\boldsymbol{R}}_{yy} = \frac{1}{N_s}\sum\nolimits_{i=1}^{N_s} \boldsymbol{Y}\boldsymbol{Y}^{\mathrm{H}} \tag{10}$$

The eigendecomposistion of $\hat{\boldsymbol{R}}_{yy}$ from (10) leads to

$$\hat{\boldsymbol{R}}_{yy} = \hat{\boldsymbol{E}}_s\hat{\boldsymbol{\Lambda}}_s\hat{\boldsymbol{E}}_s^{\mathrm{H}} + \hat{\boldsymbol{E}}_n\hat{\boldsymbol{\Lambda}}_n\hat{\boldsymbol{E}}_n^{\mathrm{H}} \tag{11}$$

where $\hat{\boldsymbol{E}}_s = [\hat{\boldsymbol{e}}_1, \hat{\boldsymbol{e}}_2, \ldots, \hat{\boldsymbol{e}}_K]$ is the signal subspace, $\hat{\boldsymbol{E}}_n = [\hat{\boldsymbol{e}}_{K+1}, \hat{\boldsymbol{e}}_{K+2}, \ldots, \hat{\boldsymbol{e}}_{M+1}]$ is the noise subspace, $\hat{\lambda}_k$ and $\hat{\boldsymbol{e}}$ are the eigenvalues and eigenvectors of $\hat{\boldsymbol{R}}_{yy}$, respectively, having the relationship $\hat{\lambda}_1 > \hat{\lambda}_2 > \cdots > \hat{\lambda}_K$.

$$\hat{\boldsymbol{\Lambda}}_s = \mathrm{diag}\{\hat{\lambda}_1, \hat{\lambda}_2, \ldots, \hat{\lambda}_K\}$$

$$\hat{\boldsymbol{\Lambda}}_n = \mathrm{diag}\{\hat{\lambda}_{K+1}, \hat{\lambda}_{K+2}, \ldots, \hat{\lambda}_{M+1}\}$$

We stress also that, the RD steering vector $\tilde{\boldsymbol{a}}(\theta_k) = \boldsymbol{W}^{\mathrm{T}}\boldsymbol{a}(\theta_k)$ is orthogonal to the columns of the noise space matrix $\hat{\boldsymbol{E}}_n$ [5–8] and proportional to the columns of the signal subspace $\hat{\boldsymbol{E}}_s$.

3 Full-azimuth DoAs estimation with the proposed UCCA shape

In this section, we will explain how we can adapt this new shape of ESPAR antennas to the ESPRIT algorithm to ensure full azimuth DoAs estimation. In fact, the estimation failure problem that prohibits the full azimuth DoAs estimation, when the azimuth angles are between 70° and 90° or between 0° and 30°, can be solved in two steps. First, we apply directly the RD-ESPRIT algorithm to estimate the DoAs of incoming sources in both upper and lower halves of the azimuth plane and all estimates are taken as a DoAs estimate candidates in this step. Second, a modified MUSIC selection function can be employed to extract the best suitable estimate among them. Hereinafter, the number of sources K is assumed to be known or has been perfectly estimated by the akaike information criterion (AIC) or minimum description length (MDL) criterion addressed in [9]. The frequency weighted matrix $\boldsymbol{W}$ is assumed full rank for the chosen reactance sets and perfectly known or obtained through experimental measurement or calculated using (7) jointly with a mutual impedance extraction technique [10].

3.1 DoAs candidate estimation step

It begins by estimating the signal subspace $\hat{\boldsymbol{E}}_s$ and compensating the coupling effect to form the processed signal subspace $\hat{\boldsymbol{E}}_s$ as

$$\hat{\tilde{\boldsymbol{E}}}_s = (\boldsymbol{W}^{\mathrm{T}})^{\dagger}\hat{\boldsymbol{E}}_s,\ \in \mathbb{C}^{(M+1)\times K} \tag{12}$$

Then, using the selection matrices $\boldsymbol{J}_i$ ($i = 1, 2$), matrices $\hat{\boldsymbol{E}}_{s1}$ and $\hat{\boldsymbol{E}}_{s2}$ are formed in accordance with the elements of each subarray. These selection matrices, composed of 1s and 0s, are used to pick up the four elements of the circular-shaped subarrays 1 and 2, respectively, among the seven array elements.

$$\hat{\boldsymbol{E}}_{si} = \boldsymbol{J}_i\hat{\tilde{\boldsymbol{E}}}_s \tag{13}$$

Once both matrices $\hat{\boldsymbol{E}}_{s1}$ and $\hat{\boldsymbol{E}}_{s2}$ are formed, total least square solution (TLS)-ESPRIT algorithm is used to estimate the spatial frequencies $\hat{\mu}_k$ and the DoAs are obtained from them as

$$\theta_k = \sin^{-1}\left(\left(\frac{\lambda}{2\pi r}\right)\hat{\mu}_k\right) + \theta_{\mathrm{r}} \tag{14}$$

If we assume that $\|\Delta\| = r = \lambda/4$, so that $\mu_k = \pi/2\sin(\theta_k - \theta_r)$. In this case, we can find a one-to-one mapping between $-1 \leq \sin(\theta_k - \theta_r) \leq 1$, corresponding to the range of possible sinus function values and $-90^\circ \leq \theta_k - \theta_r \leq 90^\circ$. Thus, the possible estimated DoAs range is given as: $0^\circ \leq \theta_k \leq 180^\circ$ and, otherwise, we prove analytically the full half azimuth coverage capability of our ESPAR antennas shape.

3.2 DoAs selection step

From the previous subsection, it is clear that the proposed ESPAR antennas shape can provide DoAs estimation only in the full upper azimuth plane [0°–180°]. Let $\hat{\boldsymbol{\Theta}}^U = [\hat{\theta}_1^U, \hat{\theta}_2^U, \cdots, \hat{\theta}_K^U]$ be these DoAs candidate provided from the upper azimuth plane. The DoAs

doi: 10.1049/iet-map.2011.0492

candidate provided from the lower half-azimuth plane [180°–360°], denoted by $\hat{\boldsymbol{\Theta}}^{\mathrm{L}} = [\hat{\theta}_1^{\mathrm{L}}, \hat{\theta}_2^{\mathrm{L}}, \cdots, \hat{\theta}_K^{\mathrm{L}}]$, can be obtained by applying the ESPRIT algorithm again but with the opposite invariance translation direction ($-\boldsymbol{\Delta}$). However, because of the symmetric geometry of the proposed antennas shape along the x-axis, the DoAs candidates estimated from the lower azimuth plane $\hat{\boldsymbol{\Theta}}^{\mathrm{L}}$ can be taken directly from (14), but with $(-\hat{\mu}_k)$ and $\theta_r + \pi$ instead of $\hat{\mu}_k$ and θ_r. So, instead of applying the ESPRIT algorithm twice (in order to cover the upper and the lower halves of azimuth plane), we estimate only the spatial frequencies $\hat{\mu}_k$ from the upper half-azimuth plane and all components of the estimated DoAs candidate vector $\hat{\boldsymbol{\Theta}}_{\mathrm{Condi}}$ (for $k = 1$ to K) will be given as follows

$$\begin{cases} \hat{\theta}_k^{U} = \sin^{-1}\left(\left(\dfrac{\lambda\hat{\mu}_k}{2\pi r}\right)\right) + \theta_{\mathrm{r}} \\ \hat{\theta}_k^{L} = \sin^{-1}\left(\left(-\dfrac{\lambda\hat{\mu}_k}{2\pi r}\right)\right) + \theta_{\mathrm{r}} + \pi \end{cases} \tag{15}$$

Once we have all components of the estimated DoAs candidate vector $\hat{\boldsymbol{\Theta}}_{\mathrm{Condi}} = [[\hat{\boldsymbol{\Theta}}^{U}][\hat{\boldsymbol{\Theta}}^{L}]]$, we focus to pick out the most appropriate DoAs among the already estimated candidates through the following selection function

$$F(\hat{\theta}_k) = \frac{\tilde{\boldsymbol{a}}(\hat{\theta})^{\mathrm{H}}\hat{\boldsymbol{E}}_s\hat{\boldsymbol{E}}_s^{\mathrm{H}}\tilde{\boldsymbol{a}}(\hat{\theta})}{\tilde{\boldsymbol{a}}(\hat{\theta})^{\mathrm{H}}\hat{\boldsymbol{E}}_n\hat{\boldsymbol{E}}_n^{\mathrm{H}}\tilde{\boldsymbol{a}}(\hat{\theta})} \tag{16}$$

where $\tilde{\boldsymbol{a}}(\hat{\theta}_k) = \boldsymbol{W}^{\mathrm{T}}\boldsymbol{a}(\theta_k)$ and $\boldsymbol{a}(\hat{\theta}_k)$ is the antenna-steering vector for the estimated DoA $\hat{\theta}_k$.

The numerator of (16) is the signal strength estimate towards $\hat{\theta}_k$. However, the denominator of (16) is the denominator of the RD-MUSIC [5] spectrum function. The above selection function is chosen to allow high discrimination between the estimated candidates. We should point out, here, that the selection function in (16) is only used to pick out certain estimations among the set of DoAs candidates. Therefore the estimation precision is determined by the precision of the ESPRIT not by the selection function $F(\hat{\theta}_k)$.

4 Computational complexity analysis

In this section, we will make a careful analysis of the required number of multiplications by the ESPRIT algorithm for DoAs estimation. During this analysis, we call UCCA-RD-ESPRIT algorithm the resulting ESPRIT algorithm applied in conjunction with the UCCA and the uniform hexagonal array (UHA)-RD-ESPRIT algorithm the resulting ESPRIT algorithm applied in conjunction with the UHA. The computational cost of both algorithms is compared with respect to their required specific operations such as the multiplications in the case of SVD and the size of the finite search space in the case of a search over a finite space. Through our analysis we will use the following three simple rules:

- The multiplication of an $(\boldsymbol{M} \times \boldsymbol{K})$ matrix and a $(\boldsymbol{K} \times \boldsymbol{L})$ matrix requires MKL multiplications.
- The eigendecomposistion of an $(\boldsymbol{M} \times \boldsymbol{M})$ matrix requires M^3 multiplications.
- The inversion of an $(\boldsymbol{M} \times \boldsymbol{M})$ sized full-rank matrix requires approximately M^3 multiplications.

4.1 DoAs estimation candidate step

As a first step, an SVD computation for assessing the signal subspace matrices is required in both cases: this operation takes $O(M_p + 1)^3$ flops in terms of complexity [11]. Since M_p refers to the number of used beam patterns to collect the received data, which defines the size of the covariance matrix, the computational complexity of this step increases with the number of these beam patterns. Then, an additional SVD for DoAs estimation step carried out by a TLS computation is needed: it takes $O(K^3)$ flops. UHA-RD-ESPRIT algorithm required six SVDs for TLS computation to cover the entire azimuth plane. However, in our approach, the half-azimuth plane [0°–180°] is covered using only one pair of subarrays: thus only one SVD for TLS computation is performed which allows a reduction of about 1/6 in calculation cost in this stage.

4.2 DoAs selection step

Since the computational load for the selection step is mainly related to the complexity of evaluating the selection function (15) as well as the number of the DoAs candidate, our approach reduces efficiently the computational cost in this step. Indeed, with the UHA the modified MUSIC selection function is evaluated with $6K$ DoAs candidate and the selection step involves a K peak search over a $6K$-size dimension space. However, with our UCCA only $2K$ DoAs candidates are evaluated and, therefore only K peaks search over a $2K$-size dimension space are performed. Consequently, in comparison with the UHA-RD-ESPRIT, it is obvious that our approach reduces significantly the computational cost by almost a factor of three in both substeps (evaluation of the selection function and the K-peak searching).

In the following, a comparative study in computational complexity is summarised in Table 1 where the computation type and, approximately, the number of multiplications required are listed for K incoming sources during one simulation trial. We denote by $P = 4$ the number of elements in each subarray, M_{p} the number of the used beam patterns and K_{condi} the number of estimated DoAs candidate. Since M_{p} represents the number of used radiation patterns, it may be much larger than the number of the ESPAR antennas elements and tends to dominate the complexity analysis.

A more direct comparison in calculation cost is illustrated in Fig. 2 where the percentage in calculation cost reduction is plotted as a function of both number of incoming sources and number of the used radiation patterns. The percentage reduction ratio is computed as

$$P_{\mathrm{ratio}}[\%] = \frac{\text{Multi. Numb. with the UCCA}}{\text{Multi. Numb. with the UHA}} \times 100$$

Fig. 2 shows an important reduction in computational effort achieved with our antennas shape (about 47 and 66%) with respect to the number of incoming sources. Furthermore, the calculation cost reduction is clearly appreciated when a generalised data covariance matrix with 13 radiation patterns, as in [8], is used to estimate $\hat{\boldsymbol{R}}_{yy}$ from (10). In this case, as we have mentioned above, the size of $\hat{\boldsymbol{R}}_{yy}$ increases and the complexity to perform the required operations for DoAs estimation such as the multiplication, the full inversion and especially the SVDs increases as well. In the same way, when the number of estimated DoAs is up to

Table 1 Computational complexity comparison of the RD-ESPRIT algorithm using the UCCA and the UHA

Operations	UCCA-RD-ESPRIT number of multiplications	Enhanced RD-ESPRIT number of multiplications
$\boldsymbol{E}_s = EVD(\boldsymbol{R}_{yy})$	M_p^3	M_p^3
$\tilde{\boldsymbol{E}}_s = (\boldsymbol{W}^T)^{\dagger}\boldsymbol{E}_s$	M_p^2K	M_p^2K
$\boldsymbol{E}_{si} = \boldsymbol{J}_i\tilde{\boldsymbol{E}}_s$	$2(PM_pK)$	$6(PM_pK)$
$\boldsymbol{E} = \begin{bmatrix} \boldsymbol{E}_{s1}^H \\ \boldsymbol{E}_{s2}^H \end{bmatrix}[\boldsymbol{E}_{s1} \quad \boldsymbol{E}_{s2}]$	$4P^2K$	$12P^2K$
$\boldsymbol{\Psi} = -\boldsymbol{E}_{12}\boldsymbol{E}_{22}^{-1}$	$2K^3$	$6K^3$
$\{v_1, v_2, \ldots, v_K\} = \text{SVD}(\boldsymbol{\Psi})$	K^3	$3K^3$
selection step	$K_{condi}[M_p(2M_{p+1}) + 1]$	$K_{condi}[M_p(2M_{p+1}) + 1]$
total number of multiplications*	$\boldsymbol{M_p}[\boldsymbol{M_p}(\boldsymbol{M_p} + \boldsymbol{K} + 2\boldsymbol{K_{condi}}) + 8\boldsymbol{K} + \boldsymbol{K_{condi}}] + \boldsymbol{K}(3\boldsymbol{K}^2 + \mathbf{16}) + \boldsymbol{K_{condi}}$	$\boldsymbol{M_p}[(\boldsymbol{M_p} + \boldsymbol{K} + 2\boldsymbol{K_{condi}}) + \boldsymbol{K}) + \mathbf{24}\boldsymbol{K_{condi}} + \boldsymbol{K_{condi}}] + \boldsymbol{K}(\mathbf{195} + \mathbf{9}\boldsymbol{K}^2) + \boldsymbol{K_{condi}}$

* $K_{condi} = 2K$ for the UCCA shape and $K_{condi} = 6K$ for the UHA shape

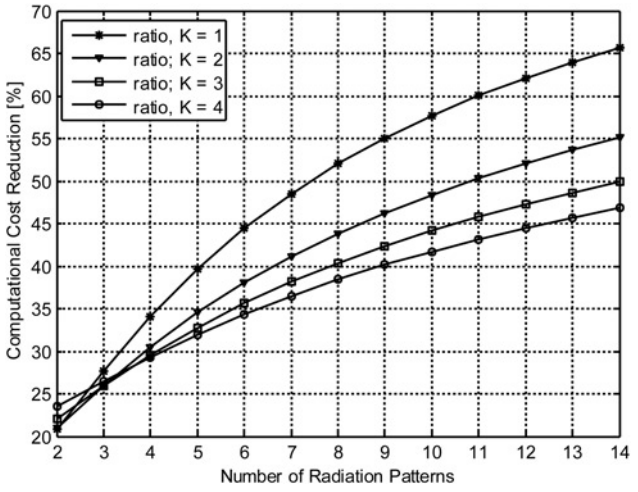

Fig. 2 *Percentage in calculation cost reduction as a function of the number of incoming sources and the number of radiation patterns*

four we show a significant reduction in the number of required multiplications which may allow significant computation-speed increase with our ESPAR antennas shape.

5 Simulation results and discussions

To demonstrate the effectiveness on DoAs estimation of the proposed array geometry, we have performed several simulation experiments to validate our approach. Whereby, we investigate the estimation errors obtained by applying the RD-ESPRIT algorithm using the UHA shape [6] and with our proposed UCCA array geometry. For RD-signal processing technique, more data covariance matrix estimation errors are brought by the directive radiation patterns, which can be viewed as a natural price of the ESPAR antennas advantages compared with the conventional antenna systems as already mentioned in the Introduction. Therefore it is very important to verify the ability of our ESPAR antennas shape to form such directive radiation patterns. An example of the resulting empirical radiation patterns are plotted as a function of the azimuth direction angles in Fig. 3. We can clearly see that the UCCA shape is able to form directive radiation patterns compared to the UHA. However, it is suitable to optimise these radiation patterns to reduce their side lobes, which will enhance further the DoAs estimation performances. Therefore more efficient sets of reactance could be found since the ESPAR antenna exhibits greater steerability control by means of its electronically controllable reactance. Nevertheless, this is a difficult task because of the particular structure of the introduced ESPAR antennas.

5.1 Performances evaluation of the proposed array geometry

To study the precision on DoAs estimation brought by this new shape of ESPAR antennas, we use as performance parameters the mean-square error (MSE) and the root-mean-square error (RMSE) defined as

$$\text{MSE}(\hat{\theta}_k) = \frac{1}{N_s}\sum_{n=1}^{N_s}(\hat{\theta}_k - \theta_k)^2 \tag{17}$$

$$\text{RMSE}(\hat{\theta}_k) = \sqrt{\text{MSE}}(\hat{\theta}_k) \tag{18}$$

where $\hat{\theta}_k$ is the estimated DoA for the ith measurement.

The simulation result, illustrated in Fig. 4, presents the variations in DoAs estimation errors (MSE) for one impinging signal according to the angles of arrival. During this simulation the signal-to-noise-ratio (SNR) level is set to 30 dB, the snapshots number is 2000 and the MSE is averaged over 1000 simulation trials. The performance on DoAs estimation with the proposed antennas shape is not affected by the sources angular positions. However, the DoAs estimation using the UHA degrades severely when the incoming signals are from some particular DoAs sectors [e.g. $(0^\circ - 25^\circ)$ and similarly $(165^\circ - 180^\circ)$]. From this simulation, it is clear that our approach gives more attractive results and provides a reliability criterion that clearly indicates whether estimations are reliable especially in these particular DoAs sectors. Therefore it is noteworthy that the used circular subarrays shape to execute the ESPRIT algorithm (instead of the lozenge shape) is a key idea to achieve an accurate DoAs estimation in the entire azimuth plane

Fig. 5 proves the multiple-signal-resolution capability of the RD-ESPRIT algorithm with the UCCA ESPAR antennas shape. It shows a single trial run for four signals DoAs estimation incoming from 55°, 85°, 210° and 355°, respectively. The SNR is set to 30 dB and 2000 snapshots are used to compute $\hat{\boldsymbol{R}}_{yy}$. Fig. 5 exhibits sharp peaks in the

doi: 10.1049/iet-map.2011.0492

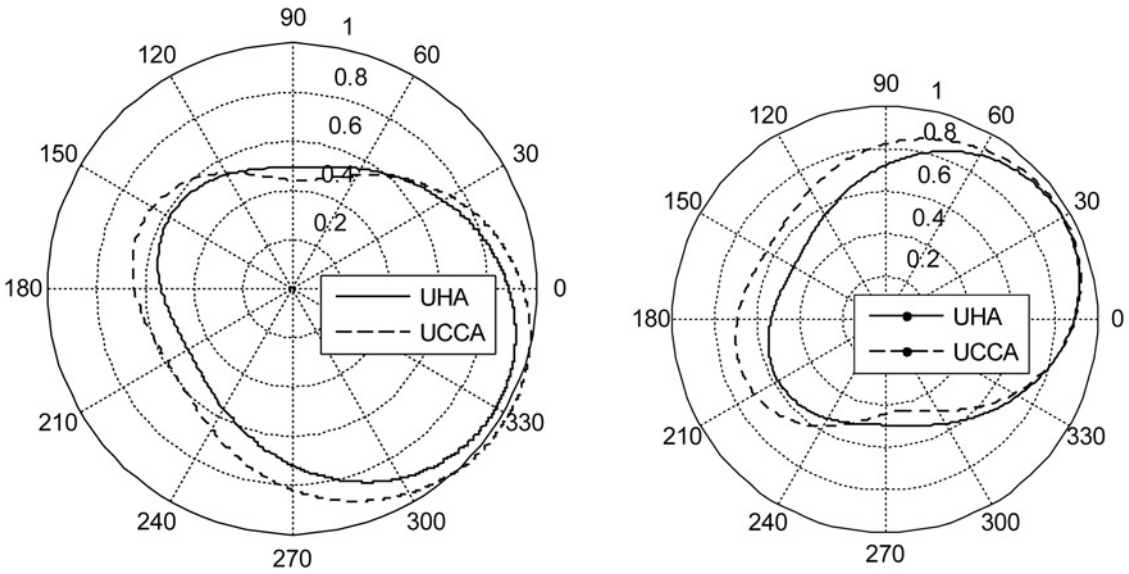

Fig. 3 *Beam patterns amplitude used for the simulation and for the numerical performance analysis of both ESPAR antennas shapes*

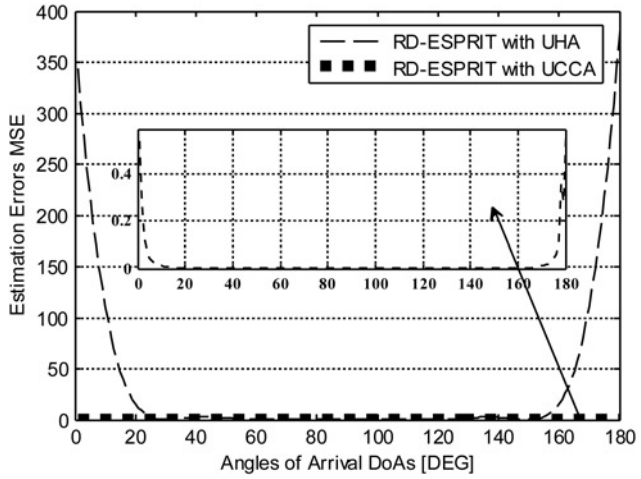

Fig. 4 *Resulting MSE against the DoAs angles obtained with both ESPAR antennas shapes*

selection function towards the true DoAs and a local minimum for the rest of DoAs candidate. It follows that our approach to select the final estimated DoAs among the already estimated candidate works efficiently.

5.2 Performances on DoAs estimation with the proposed UCCA shape

In the previous subsection, we have verified that the proposed antennas shape can perform better DoAs estimation results than the UHA in the full-azimuth plane when it is used in conjunction with the standard ESPRIT. In this subsection, we will investigate the performances on DoAs estimation achieved by the UCCA shape in some difficult scenarios.

Fig. 6 illustrates the resulting reactance domains standard deviation of the Cramer Rao bound (Std-RD-CRB) curves of both array geometries as a function of the angular separation $\Delta\theta$ when two sources impinge the ESPAR antennas from 80° and $80^\circ + \Delta\theta$, respectively. In the same figure, the resulting Std-RD-CRB curves when two other sources impinging the ESPAR antennas from 10° and $10^\circ + \Delta\theta$, respectively, are also plotted. Both simulations are performed separately and all obtained results are illustrated together and compared with the Std-CRB of both conventional antennas arrays and ESPAR antennas. During these simulations the SNR is set to 30 dB where 2000 snapshots per pattern is used to estimate $\hat{\boldsymbol{R}}_{yy}$ from (10) with 1000 simulations trials. In Fig. 6, only the Std-RD-CRB curves of the first sources at DoA $= 80^\circ$ and DoA $= 10^\circ$ are shown since the second sources at DoA $= 80^\circ + \Delta\theta$ and DoA $= 10^\circ + \Delta\theta$ will behave similarly. The goal is to highlight the performance on DoAs estimation superiority brought by the proposed antennas shape for two neighbouring sources scenario. For a very close source's DoAs ($\Delta\theta = 4^\circ$), Fig. 6 shows that the UCCA shape performs better DoAs estimation accuracy over the UHA (RMSE less than 0.4° for the source at $\theta = 80^\circ$). On the other hand, unlike the UHA shape, the obtained performances with our UCCA shape are approximately the same for both considered sources DoAs (sources at 80° and 10°). Thus, Fig. 6 clearly indicates that the UCCA shape can perform robust DoAs estimation for very close sources'

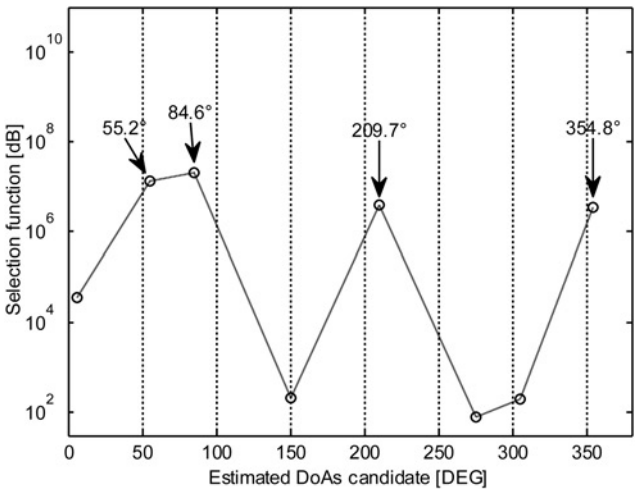

Fig. 5 *Successful example of four-signal estimation, where DoAs are toward $\theta_1 = 55^\circ$, $\theta_2 = 85^\circ$, $\theta_3 = 210^\circ$ and $\theta_4 = 355^\circ$*

Circle marks, o, represent the estimated DoAs candidates and the value of the candidates selected as the DoAs estimated (corresponding to spectrum peak values) are written in the graph

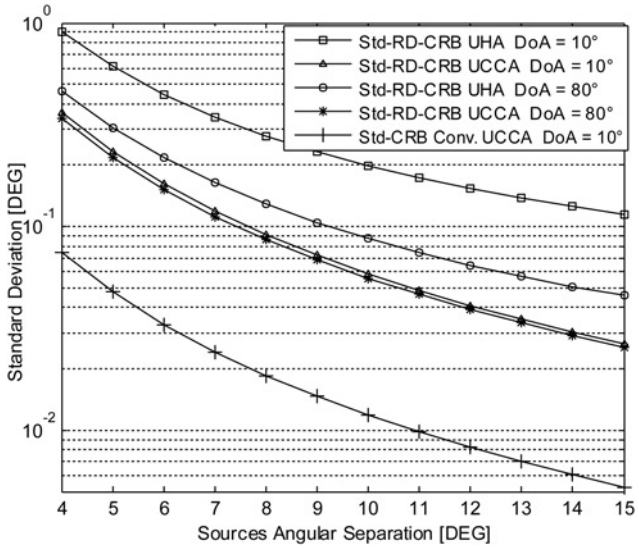

Fig. 6 *Cramer Rao bound CRB of both UHA and UCCA arrays against the sources angular separations $\Delta\theta$*

DoAs even if they are incoming from the broadside directions. Furthermore, since the CRB provides an unbeatable performance limit for any unbiased estimator, an estimator that uses the UCCA shape may yield lower estimation errors than one using the UHA shape.

To more validate our approach, it is interesting to compare the performances on DoAs estimation of the proposed UCCA-ESPAR antennas to those obtained with conventional UCCA shape. The conventional array is assumed to be perfectly calibrated, so mutual coupling effects because of $r_1 = \lambda/4$ could be neglected. The conventional antennas array gives better results than ESPAR antennas as illustrates Fig. 6. However, although such results could be expected, performances of ESPAR antennas can be considered sufficient for DoAs estimation applications in comparison with conventional arrays. Moreover, the cost reduction using only a single active receiver as well as the low-power consumption of ESPAR antennas, may outweigh their loss of performances compared to conventional arrays.

Fig. 7 depicts the resulting RMSE on DoAs estimation as a function of the SNR levels for two incoming sources from 10° and 80°, respectively. The RMSE is averaged over 2000 simulation trials where 1000 snapshots per pattern are used to compute $\hat{\boldsymbol{R}}_{yy}$ from (10). Fig. 7 shows that the estimation errors, obtained with the UCCA shape, decrease quickly as soon as the SNR level increases even when the incoming source is at 10° (less than 1° for an SNR of 10 dB). Therefore comparatively to the UHA where the achieved performances are strongly dependent on the sources' DoAs, no angle-dependency on the achieved performance is shown with the UCCA shape especially for a high SNR levels (beyond 10 dB) as Fig. 7 illustrates.

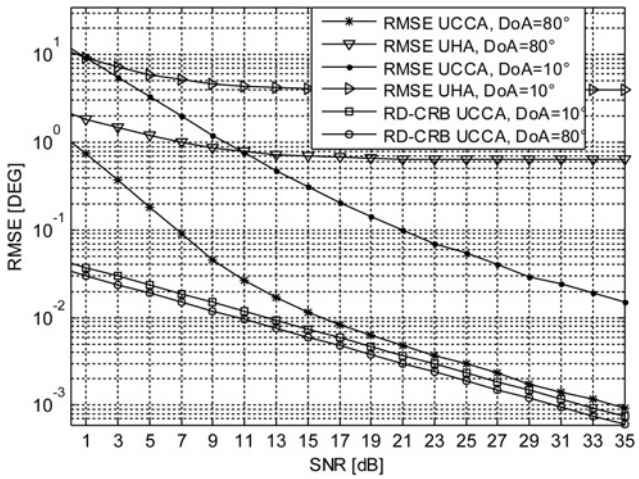

Fig. 7 *RMSE against the SNR level for two sources impinging on the UCCA antenna array from $\theta_1 = 10°$ and $\theta_2 = 80°$*

From the previous simulations, it is clear that the proposed antenna shape gives more attractive results than the classic UHA shape. This may be because of the fact that the translational invariance configurations of the UHA, used to execute the RD-ESPRIT algorithm [6], are able to estimate only the DoAs of one signal because they can resolve just the incoming signal from the nearest perpendicular direction of these translational invariance configurations.

6 Conclusion

This paper has proposed a new shape of ESPAR antennas. We have demonstrated that applying the ESPRIT algorithm in conjunction with this new shape reduces the computational load drastically and the processing time by almost a factor of three since the full-azimuth plane is covered by only one pair of subarray configuration instead of three as for the well-known hexagonal ESPAR antennas shape. Moreover, we have also explained that the use of circular-shaped subarrays to execute the ESPRIT algorithm is the key feature that can remove the drawbacks of the estimation-failure problems when sources' DoAs are far from the normal direction of the used invariance antenna configuration. Therefore the performance loss of the enhanced RD-ESPRIT algorithm relative to the UCCA-RD-ESPRIT algorithm for some sources DoAs sectors can be viewed as a natural result for the full-azimuth scan capability of the used circular-shaped subarrays. On the other hand, the proposed algorithm not only improves computational efficiency with high DoAs estimation accuracy, but also, it leads to a very efficient computational methodology required for real time implementation as on a DSP chip. Nevertheless, comparatively to linear or circular arrays, the UCCA shape has attracted little attention in DoAs estimation research field. Therefore the introduced antenna shape sheds a new light on the efficiency of the uniform concentric circular-shaped ESPAR antennas systems for DoAs estimation with high-resolution methods.

7 Acknowledgments

The authors gratefully acknowledge the contributions of reviewers and thank the anonymous reviewers for their valuable comments that significantly improved the quality of this paper.

8 References

1 Schmit, O.R.: 'Multiple emitter location and signal parameters estimation', *IEEE Trans. Antennas Propag.*, 1986, **34**, pp. 276–280
2 Roy, R., Kailath, T.: 'ESPRIT estimation of signal parameters via rotational invariance techniques', *IEEE Trans. Acoust. Speech Signal Process.*, 1989, **37**, pp. 984–995
3 Marcos, S., Marsal, A., Benidin, M.: 'The propagator method for source bearing estimation', *Signal Process.*, 1995, **42**, pp. 121–138

doi: 10.1049/iet-map.2011.0492

4 Svantessn, T., Wen, M.: 'High resolution direction finding using a switched parasitic antenna'. Proc. 11th IEEE Signal Processing Workshop on Statistical Signal Processing, Singapore, 2001, pp. 50–52
5 Plapous, C., Cheng, J., Taillefer, E., Hirata, A., Ohira, T.: 'Reactance domain MUSIC algorithm for electronically steerable parasitic array radiator antenna', *IEEE Trans. Antennas Propag.*, 2004, **52**, (12), pp. 3257–3264
6 Taillefer, E., Hirata, A., Ohira, T.: 'Reactance-domain ESPRIT algorithm for a hexagonally shaped seven-element ESPAR antenna', *IEEE Trans. Antennas Propag.*, 2005, **53**, (11), pp. 3486–3495
7 Huang, A.-M., Wan, Q., Chen, X.-X., Yang, W.-L.: 'Enhanced reactance-domain ESPRIT method for ESPAR antenna'. Proc. IEEE Region 10 Conf. TENCON, 2006, pp. 14–17
8 Taillefer, E., Nomura, W., Cheng, J., Taromaru, M., Watanabe, Y., Ohira, T.: 'Enhanced reactance-domain ESPRIT algorithm employing multiple beams and translational-invariance soft selection for direction-of-arrival estimation in the full azimuth', *IEEE Trans. Antennas Propag.*, 2008, **56**, (8), pp. 2514–2526
9 Wax, M., Kailath, T.: 'Detection of signals by information theoretic criteria', *IEEE Trans. Acoust. Speech Signal Process.*, 1985, **33**, pp. 387–392
10 Han, Q., Hanna, B., Inagaki, K., Ohira, T.: 'Mutual impedance extraction and varactor calibration technique for ESPAR antenna characterization', *IEEE Trans. Antennas Propag.*, 2006, **54**, (12), pp. 3713–3720
11 Hnarng, K.C., Yeh, C.C.: 'A unitary transformation method for angle-of-arrival estimation', *IEEE Trans. Signal Process.*, 1991, **39**, pp. 975–977